The importance of vortex bundles in quantum turbulence at absolute zero

A. W. Baggaley

Citation: Phys. Fluids **24**, 055109 (2012); doi: 10.1063/1.4719158
View online: http://dx.doi.org/10.1063/1.4719158
View Table of Contents: http://pof.aip.org/resource/1/PHFLE6/v24/i5
Published by the American Institute of Physics.

The importance of vortex bundles in quantum turbulence at absolute zero

A. W. Baggaley[a)]
School of Mathematics and Statistics, University of Newcastle, Newcastle upon Tyne, NE1 7RU, United Kingdom

(Received 22 March 2012; accepted 24 April 2012; published online 18 May 2012)

This study is concerned with the existence of coherent bundles of quantized vortices, and their importance in creating a flow with the classical Kolmogorov scaling and energy cascade. We show that at finite (non-zero) temperatures, in the presence of turbulent normal fluid, quantized vortices are organized into coherent bundles. We also performed a number of simulations at zero temperature and demonstrate that for a Kolmogorov scaling, and hence a hydrodynamical energy cascade, vortices must be organized into coherent bundles. Finally we analyze the polarization of the vortex tangle and find good agreement with theoretical predictions. © *2012 American Institute of Physics*. [http://dx.doi.org/10.1063/1.4719158]

I. INTRODUCTION

Theoretical and experimental work exploring turbulence in the quantum phases of ^{4}He, ^{3}He, and atomic Bose-Einstein condensates, so-called quantum or superfluid turbulence, has attracted a wealth of attention in recent years.[27,30] Quantum turbulence consists of a disordered tangle of thin, discrete vortex lines of quantized circulation, κ, specific to the atomic properties of the fluid. At finite (non-zero) temperatures, quantum turbulence is a complex state in which a viscous normal fluid interacts with an inviscid superfluid, via mutual friction. In the former, vorticity is unconstrained; the building blocks of the turbulence are "swirling" motions, eddies, which can take any size and strength. In the superfluid component, vorticity can only exist in the form of topological defects, quantized vortex lines, with microscopic thickness and fixed strength.

A number of experimental methods, with classical analogues, have been used to create this two-fluid turbulence in ^{4}He, for example, agitating superfluid liquid helium with propellers,[19,24] forks,[8] or grids.[28] There are also methods of generating turbulence which are unique to superfluid liquid helium, for example, heat flows,[10,29] which we do not consider here. Quantum turbulence can also be generated and studied in the more exotic isotope ^{3}He[9,11] and atomic Bose-Einstein condensates.[13]

If both the normal fluid and superfluid are turbulent, then a number of experimental[19,24,25] and numerical studies[15,23] have shown that the superfluid component exhibits the Kolmogorov spectrum, $E(k) \sim k^{-5/3}$. Numerical studies have suggested that this is due to a "locking" of the quantized vortices in the superfluid due to vortical structures within the superfluid.[15,20] In this article we add further weight to these claims, showing the existence of bundling using "synthetic" turbulence to model the motion of the normal fluid.

Numerical studies have also shown the existence of the Kolmogorov spectrum at zero temperature,[3] where the relative density of the normal fluid is zero and the system is a pure superfluid. The commonly held assumption is that the quantized vortices are organized in bundles,[17,18] which are then associated with Kolmogorov turbulence in the zero-temperature limit. Indeed these bundles have been shown to be stable structures which can survive reconnection events.[2]

[a)]Electronic mail: a.w.baggaley@ncl.ac.uk.

One possible reason for the need for vortex bundles is that they facilitate vortex stretching, an important mechanism for energy transfer, and hence the cascade, in classical turbulence.[12] Due to the fixed circulation of a quantized vortex an individual vortex line cannot be stretched; its length can change but the circulation is fixed. A bundle circumvents this and allows the quantized vortices to act like a vortex tube in a classical fluid.

The existence of bundles is expected to have a decisive impact on the the dissipation mechanism of the turbulence. In an unpolarized tangle, reconnections are believed to play the dominant role in dissipating energy at small scales. If the turbulence is polarized due to the bundles then reconnections may be suppressed, as the vortices in the bundles are close to parallel.[18] In such a system Kelvin waves, generated by either reconnections or the motion of eddies at the intervortex scale, are believed to be the dominant dissipation mechanism.[17,18] In this article we show that bundles, a local polarization of the vortices, are indeed beneficial, and perhaps necessary, in the creation of an organized flow at large scales.

II. NUMERICAL METHODS

In superfluid ^{4}He, the vortex core radius ($a_0 \approx 10^{-8}$ cm) is many orders of magnitude smaller than the average separation between vortex lines (typically from 10^{-2} to 10^{-4} cm) or any other relevant lengthscale in the flow such as the typical radius of curvature of the lines. Therefore, a common approach[26] is to model vortex lines as spaces curves $\mathbf{s} = \mathbf{s}(\xi, t)$ of infinitesimal thickness, where t is the time and ξ is arc length. In the vortex filament method these space curves are numerically discretized by a large, variable number of points $\mathbf{s}_i$ ($i = 1, \ldots, N$), which hereafter we refer to as vortex points. Constant remeshing of the filaments are required, as it is desirable to maintain a relatively constant resolution along the filaments. To this end we add or remove vortex points as the length of the filaments changes, hence N varies throughout the simulation. In a recent paper[6] we discussed the various numerical details at length, here it is suffice summarize a few key points. First we control the resolution along the filaments ensuring the separation of vortex points lies between an upper, δ, and lower, $\delta/2$, bound. Second we impose the reconnections of filaments, reconnecting separate filaments if the distance between them is less than $\delta/2$. The motivation to enforce reconnections is due to both experimental[22] and numerical[16] observations that superfluid vortex lines can reconnect with each other when they come sufficiently close. Importantly we have confirmed[5] that the vortex filament method is relatively insensitive to the reconnection procedure used.

The motion of a vortex filament, and hence the vortex points in the numerical model, is determined by the normal fluid, through mutual friction, and by the induced velocity of the other vortices. The governing equation of motion of the superfluid vortex lines at point $\mathbf{s}$ is given by the Schwarz equation[26]

$$\frac{d\mathbf{s}}{dt} = \mathbf{v}_s + \alpha \mathbf{s}' \times (\mathbf{v}_n - \mathbf{v}_s) - \alpha' \mathbf{s}' \times \left[\mathbf{s}' \times (\mathbf{v}_n - \mathbf{v}_s)\right], \tag{1}$$

where α, α' are temperature dependent friction coefficients,[7] $\mathbf{v}_n$ is the normal fluid's velocity field, and $\mathbf{v}_s$ is the superfluid's velocity field. Here the prime denotes derivative with respect to arclength, e.g., $\mathbf{s}' = d\mathbf{s}/d\xi$. As is common in the literature[1,14,20] we prescribe the normal flow, ignoring any back-reaction of the quantized vortices on the normal fluid. We take $\alpha = 0.5$ and $\alpha' = -0.03$, corresponding to a temperature of 1.9 K.

In our system the quantized vortices define the vorticity field; we recover the velocity field $\mathbf{v}_s$ by numerically solving the Biot-Savart (BS) integral

$$\mathbf{v}_s(\mathbf{s}) = -\frac{\kappa}{4\pi} \oint_{\mathcal{L}} \frac{(\mathbf{s} - \mathbf{r})}{|\mathbf{s} - \mathbf{r}|^3} \times \mathbf{dr}, \tag{2}$$

where the line integral extends over the entire vortex configuration $\mathcal{L}$. Here $\kappa = h/m$ is the quantum of circulation, where h is Planck's constant and m is the mass of a ^{4}He atom. The integral can be desingularized in a standard way.[26] To speed up the computation of the BS integral we make use of a

tree approximation, specific details can be found in Ref. 4, here it is sufficient to state that the critical opening angle $\theta_{\max} = 0.4$, reducing the evaluation of the BS integral from an $\mathcal{O}(N^2)$ procedure to $\mathcal{O}(N \log(N))$.

All simulations are performed within a cube of size $D = 0.1$ cm with periodic boundary conditions. When evaluating the tree approximation to the BS integral, Eq. (2), for each vortex point in the box we consider the other $3^3 - 1 = 26$ boxes around it through periodic wrapping. In all simulations we use parameters which refer to ^{4}He, circulation $\kappa = 9.97 \times 10^{-4}$ cm^2/s and vortex core radius $a_0 = 10^{-8}$ cm. We take $\delta = 2 \times 10^{-3}$ cm and use a numerical timestep of 5×10^{-5} s, sufficient to resolve Kelvin waves at scales corresponding to $\delta/2$. Spacial derivatives, which arise in evaluating the local part of the desingularized BS equation, are approximated using 4th order finite-difference scheme. Finally timestepping is performed using a 3rd order Adams–Bashforth scheme.

III. KOLMOGOROV TURBULENCE AT FINITE TEMPERATURES

The viscosity of the normal fluid is small in ^{4}He, therefore, if quantum turbulence is driven by mechanical means, we would expect the normal fluid to be turbulent. To model the turbulent normal fluid we use the kinematic simulation (KS) model,[21] in which the normal fluid velocity at position $\mathbf{s}$ and time t is prescribed by the following sum of M random, unsteady Fourier modes:

$$\mathbf{v}_n(\mathbf{s}, t) = \sum_{m=1}^{M} \left(\mathbf{A}_m \times \mathbf{k}_m \cos\phi_m + \mathbf{B}_m \times \mathbf{k}_m \sin\phi_m\right), \tag{3}$$

with $\phi_m = \mathbf{k}_m \cdot \mathbf{s} + \zeta_m t$, where $\mathbf{k}_m$ and $\zeta_m = \sqrt{k_m^3 E(k_m)}$ are wavevectors and frequencies. Via an appropriate choice of $\mathbf{A}_m$ and $\mathbf{B}_m$, the energy spectrum of $\mathbf{v}_n$ reduces to the Kolmogorov form $E(k_m) \propto k_m^{-5/3}$ for $1 \ll k \ll k_M$, with $k = 1$ at the integral scale and k_M at the cut-off scale. The effective Reynolds number $\mathrm{Re}_n = (k_M/k_1)^{4/3}$ is defined by the condition that the dissipation time equals the eddy turnover time at $k = k_M$. We have adapted Eq. (3) to periodic boundary conditions, by ensuring a 2π dependence in the components of $\mathbf{k}_m$. Hence, $\mathbf{v}_n$ is a convenient model for homogeneous isotropic turbulence in an incompressible fluid. Figure 1 displays a two-dimensional slice of the velocity field used in this study.

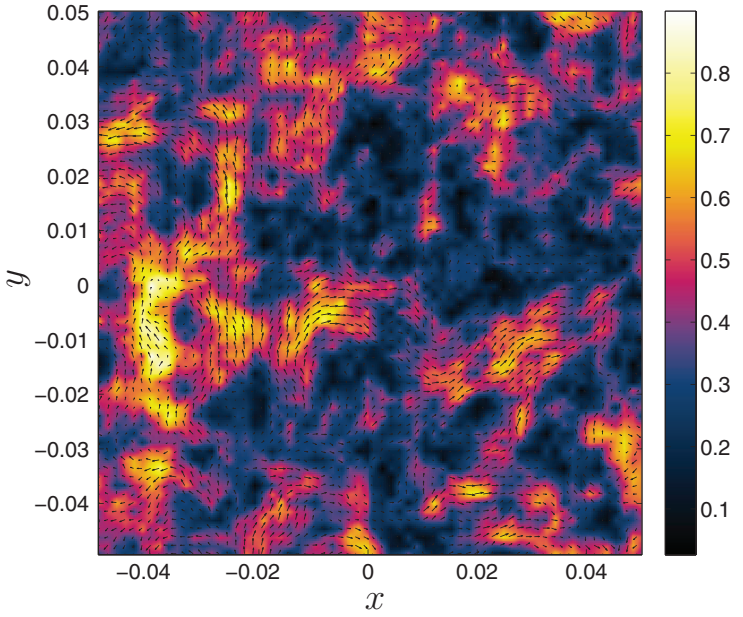

FIG. 1. Slice in the xy-plane ($z = 0$) of the normal fluid velocity $\mathbf{v}_n$ using the KS flow Eq. (3) with $M = 188$ and $\mathrm{Re}_n \approx 200$. The slice is colored according to the modulus of the velocity field.

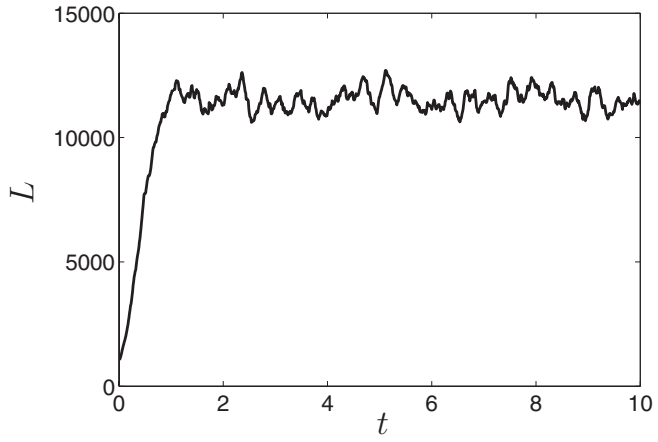

FIG. 2. The vortex line density L (cm^{-2}), plotted as a function of time t (s), for the finite temperature simulation driven by the KS flow Eq. (3).

For the simulations presented here we take $M = 188$, $k_1 = 0.1$ cm, and $k_M = 1.8 \times 10^{-3}$ cm, which gives $\mathrm{Re}_n \approx 200$. The initial conditions for the quantized vortices are a set of 100 randomly oriented vortex rings with radius 9.5×10^{-3} cm. We timestep the vortices, according to Eq. (1), for a period of 10 s, approximately 25 large eddie turnover times for the normal fluid. A time series of the evolution of the vortex line density $L = \Lambda / V$ (Λ is the total length of the vortices and $V = D^3$ is the volume of the cubic domain) is displayed in Fig. 2. Initially there is a rapid growth in the vortex line density, until the energy injected from the normal fluid is balanced by dissipation due to vortex reconnections, after which L fluctuates around a mean value. In this steady state we analyze both the energy spectrum of the superfluid velocity field and the structure of the vortices. Figure 3 (left) shows the vortex tangle at $t = 10$s, the energy spectrum, averaged over the saturated part of the simulation ($2\,\mathrm{s} \leq t \leq 10\,\mathrm{s}$), is displayed in Fig. 3 (middle). To compute the energy spectrum we construct a 512^2 mesh in the xy-plane at the center of the box ($z = 0$). At each mesh point we calculate $\mathbf{v}_s$, using the tree approximation to the BS integral Eq. (2).

We display this spectrum in Fig. 3 and note that it is consistent with Kolmogorov scaling at low k. The pertinent question is: are there also associated bundles of quantized vortices? Visual inspection of the vortex tangle may suggest bundles; however, we seek more quantitative evidence of there existence. We convolve the discrete vortex filaments with a Gaussian kernel, and define a

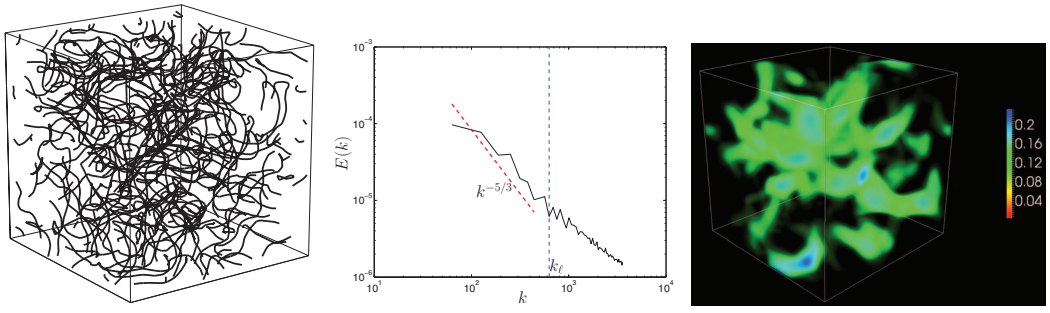

FIG. 3. The left panel shows the vortex tangle produced in the simulation at finite temperature where the normal fluid velocity is the prescribed KS flow Eq. (3), at $t = 10$ s. The middle panel displays the energy spectrum $E(k)$ vs the wavenumber k (cm^{-1}), note that the vertical dashed line corresponds to the intervortex spacing k_ℓ. (Right) A volume rendering of the smoothed vorticity field $\boldsymbol{\omega}$ (s^{-1}) computed on a 128^3 cartesian mesh.

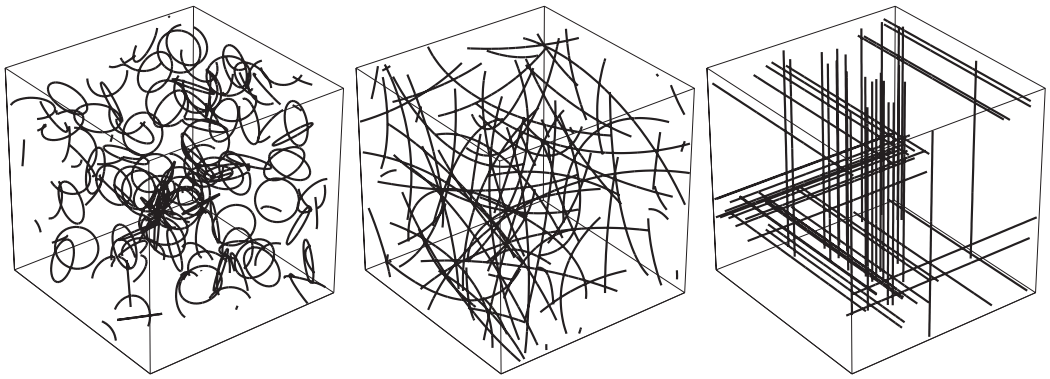

FIG. 4. The initial conditions for the three simulations performed at 0 K. (Left) 100 randomly oriented an positioned loops of radius 9.5×10^{-3} cm, (middle) 10 loops of radius 9.55×10^{-2} cm, and (right) 60 randomly oriented and directed lines arranged into bundles of 2 with a typical separation of 4×10^{-3} cm.

smoothed vorticity field $\boldsymbol{\omega}$, on a regular Cartesian mesh

$$\boldsymbol{\omega}(\mathbf{r},\ t) = \kappa \sum_{i=1}^{N} \frac{\mathbf{s}_i'}{(2\pi\sigma^2)^{3/2}} \exp(-|\mathbf{s}_i - \mathbf{r}|^2/2\sigma^2)\Delta\xi\ , \tag{4}$$

where $\mathbf{s}_i' = d\mathbf{s}_i/d\xi$ is the unit vector along a vortex at $\mathbf{s}_i = \mathbf{s}_i(\xi, t)$ and N is the number of discretization points. We choose a smoothing length σ which is of the order of $\ell = 1/\sqrt{L}$, the typical separation of vortices, commonly referred to as the intervortex spacing. This is the only relevant lengthscale to smooth over.

Figure 3 (right) shows a volume rendering of the smoothed vorticity field $\boldsymbol{\omega}$ computed on a 128^3 grid. Strong vortical regions are visible, which we associate with coherent bundles of vortices. This provides further evidence,[15,20] that Kolmogorov turbulence in the superfluid component, at finite temperatures is associated with bundles of vortices. The key question is: is this true at zero temperature and are bundles necessary?

IV. TURBULENCE AT ZERO TEMPERATURE

As previously discussed, at zero temperature the system is a pure superfluid; hence, the equation of motion for a vortex point reduces to

$$\frac{d\mathbf{s}}{dt} = -\frac{\kappa}{4\pi} \oint_{\mathcal{L}} \frac{(\mathbf{s} - \mathbf{r})}{|\mathbf{s} - \mathbf{r}|^3} \times \mathbf{dr}. \tag{5}$$

Our aim is to see if bundling of vortices is necessary for a Kolmogorov spectrum. With this in mind we consider three different initial conditions. First we consider a system comprises 100 randomly oriented and positioned loops of radius 9.5×10^{-3} cm, see Fig. 4 (left). We evolve the system for a period of 0.5 s and then examine the energy spectra and smoothed vorticity field, $\boldsymbol{\omega}$. These are displayed in Fig. 5 along with a snapshot of the final state of the vortex tangle.

Clearly here there is no large scale flow and no bundles are present. This is due to the fact that the initial configuration contained little energy at large scales. Motivated by this we consider again a system of loops but with a radius of the order of the domain size. In order to maintain the same initial vortex line density we use 10 loops of radius 9.55×10^{-2} cm. After the application of periodic boundary conditions this leaves a system of nearly straight vortices which have random positions and orientations, Fig. 4 (middle). We verify that here the bulk of the energy is contained in large scale motions. Again we timestep the system for 0.5 s and compute the energy spectra and smoothed vorticity field, see Fig. 6. As before we see no formation of the Kolmogorov spectra and the spectrum corresponds to that of a non-cascading straight vortex $E(k) \sim k^{-1}$. If we inspect the smoothed vorticity field we again see a lack of bundles or coherent structures.

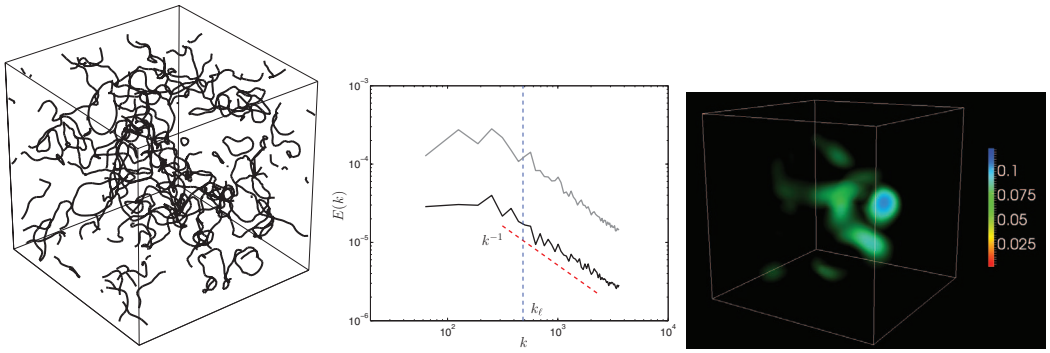

FIG. 5. (Left) The vortex tangle after 0.5 s resulting from small vortex loops, Fig. 4 (left). (Middle) The energy spectrum $E(k)$ vs the wavenumber k (cm^{-1}), note that the vertical dashed line corresponds to the intervortex spacing k_ℓ. The initial energy spectrum is displayed as a grey line. (Right) A volume rendering of the smoothed vorticity field, due to this vortex configuration, computed on a 128^3 Cartesian mesh.

Finally we consider a system where we seek to promote bundling of the quantized vortices. We take a set of 15 straight vortex lines, randomly oriented and directed along either the x, y, or z axis. For each initial line we create a three further parallel vortex lines, oriented in the same direction, but with its location offset by the initial intervortex spacing, approximately 5δ, leading to bundles of four vortices. This initial condition is seen in Fig. 4 (right). Note that the choice of 60 lines ensures the total vortex line density is approximately the same as in the two loop simulations. As in the previous two simulations, we timestep the system for 0.5 s and compute the energy spectra and smoothed vorticity field, see Fig. 7. Agreement with the Kolmogorov spectrum is visible at lengthscales larger than the intervortex spacing. Associated with this we see coherent structures in the smoothed vorticity field, which we associate with organized bundles of vortices. In order to display the arrangement of vortices which leads to such a structure in Fig. 8 we display a magnified section of the tangle corresponding to an intense vortical region.

In all zero-temperature simulations the energy spectrum is computed from the final vortex configuration on a 512^2 mesh in the xy-plane ($z = 0$). As earlier the smoothed vorticity field $\boldsymbol{\omega}$ is visualized from a 128^3 mesh. Due to the inherent randomness of these initial conditions we perform a large number of simulations and our conclusions remain robust to different configurations of loops or lines. We have also confirmed that changing the degree to which the vortices are bundled in the 3rd simulation does not dramatically change the results of the simulation. However if the spacing between the two vortices in the 'bundle' is very large, which can result in straight vortices with no evidence of bundling, then we see the k^{-1} spectrum due to a straight vortex.

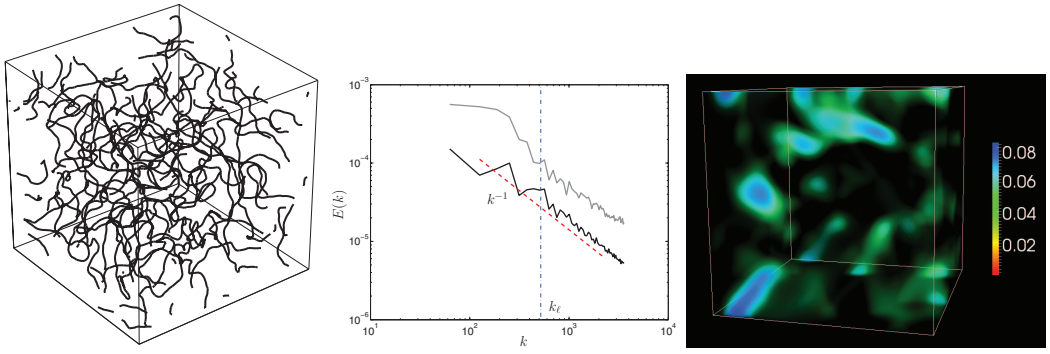

FIG. 6. (Left) The vortex tangle after 0.5 s resulting from large vortex loops, Fig. 4 (middle). (Middle) The energy spectrum $E(k)$ vs the wavenumber k (cm^{-1}), note that the vertical dashed line corresponds to the intervortex spacing k_ℓ. The initial energy spectrum is displayed as a grey line. (Right) A volume rendering of the smoothed vorticity field, due to this vortex configuration, computed on a 128^3 Cartesian mesh.

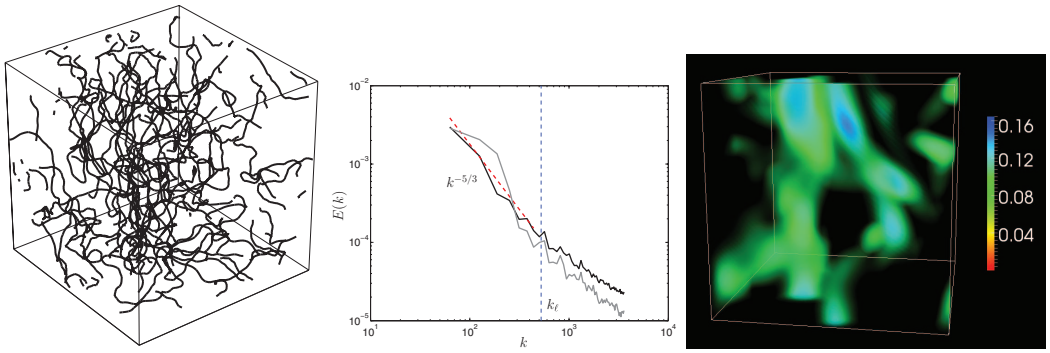

FIG. 7. (Left) The vortex tangle after 0.5 s resulting from bundled vortex lines, Fig. 4 (right). (Middle) The energy spectrum $E(k)$ vs the wavenumber k (cm^{-1}), note that the vertical dashed line corresponds to the intervortex spacing k_ℓ. The initial energy spectrum is displayed as a grey line. (Right) A volume rendering of the smoothed vorticity field, due to this vortex configuration, computed on a 128^3 Cartesian mesh.

In all plots of the energy spectra (Figs. 5–7, middle panel) we also include the initial energy spectra, plotted in grey. In the simulations which do not exhibit agreement with the Kolmogorov spectrum, Figs. 5 and 6, a much greater decrease in energy is seen, compared to Fig. 7. This supports the hypothesis that the bundling of vortices leads to a suppression of reconnections.[18] This would explain the noticeably lower reduction in the energy of the system seem in Fig. 7. We plan to investigate this behaviour further in a future study. Finally in Fig. 7 we note a prominent increase in the energy at scales below the intervotex spacing, k_ℓ, due to the Kelvin wave cascade.

A. Polarization of the tangle

In the work of L'vov *et al.*,[18] the polarization of the tangle was quantified by defining the circulation $\Gamma(R)$ over a contour of a two–dimensional disc of radius R. Vortices will intersect this

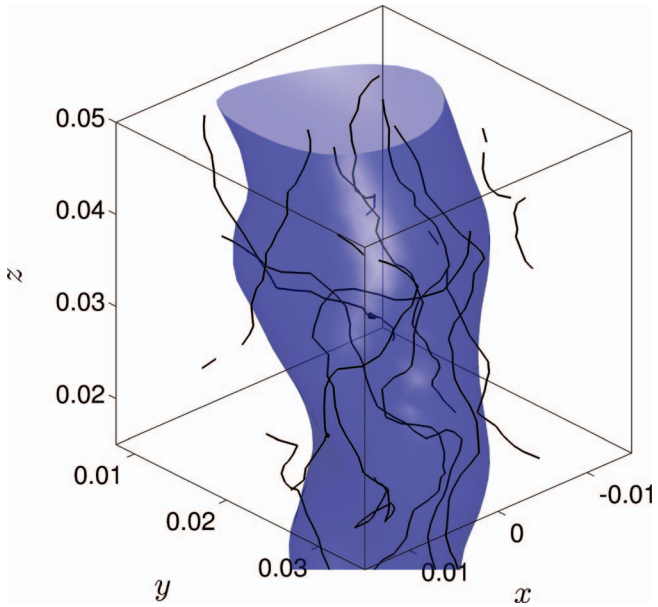

FIG. 8. A magnified plot of a single structure from the zero-temperature simulation which exhibits the Kolmogorov scaling (Fig. 7), plotted at $t = 0.5$ s. We plot only the vortex segments that make up the structure as black lines. An isosurface of the smoothed vorticity field is plotted at 2.3 $\omega_{\rm rms}$, $\omega_{\rm rms} = 0.065$.

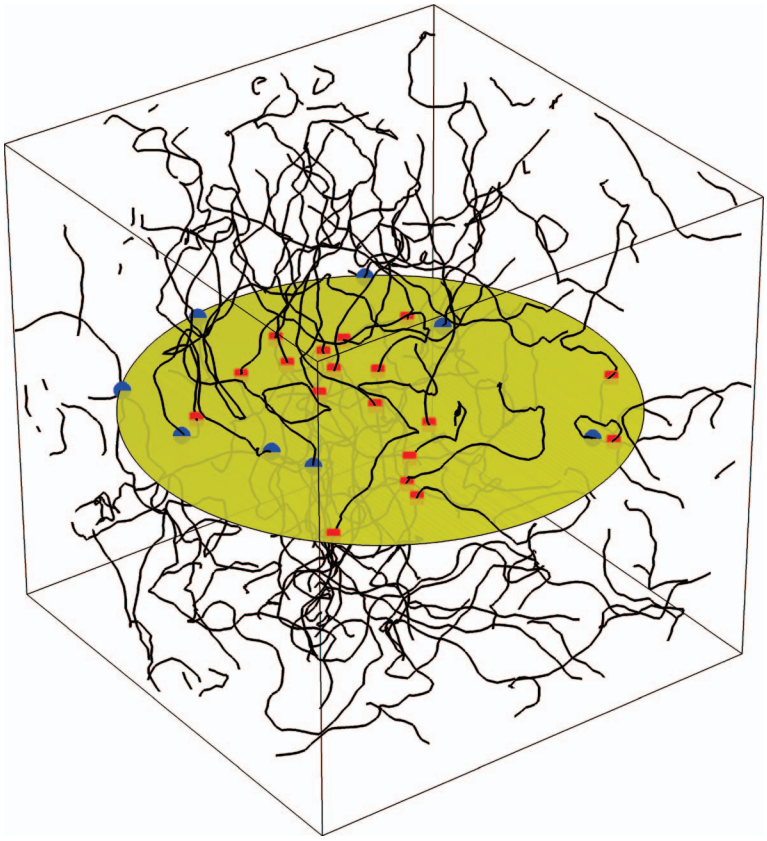

FIG. 9. A disc of radius $D/2$ in the xy-plane ($z = 0$) from which Γ, Eq. (6), can be computed. Positive crossings of the disc are plotted as (red) squares and negative crossings are plotted as (blue) circles.

disc, in both the positive and negative direction, and $\Gamma(R)$ is given by

$$\Gamma(R) = \kappa(N_+ - N_-). \tag{6}$$

If we can assume the following scaling:

$$\langle \Gamma^2 \rangle = \kappa^2 (R/\ell)^\sigma, \tag{7}$$

then L'vov *et al.*[18] showed that an unpolarized tangle has $\sigma = 2$, and a tangle with the Kolmogorov spectrum should have $\sigma = 8/3$. We test these predictions by creating 10 000 random discs, of radius $D/2$ and counting the number of positive and negative crossing through the disc, to compute Γ^2. Figure 9 shows an example of such a disc in the xy-plane at $z = 0$.

From this we estimate $\sigma = 1.8$ in the simulation with random loops of radius 9.55×10^{-2} cm (Fig. 6) which exhibits the $E(k) \sim k^{-1}$ scaling. In the simulation with enforced bundling (Fig. 7), which does display the Kolmogorov scaling, we estimate $\sigma = 2.6$.

V. CONCLUSIONS

We have shown that at finite temperature quantum turbulence driven by a turbulent normal fluid exhibits both the Kolmogorov spectrum and a characteristic bundling of vortices.

We have performed a large number of numerical simulations at zero temperature, presenting three pertinent examples in the text. What is clear from these simulations is that bundles of vortices are needed in order to see the Kolmogorov spectrum, $E(k) \sim k^{-5/3}$. In simulations with energy at large scales, but with no local polarization or bundling of vortices, the energy spectrum $E(k) \sim k^{-1}$, corresponding to a straight vortex. We also show that theoretical predictions[18] regarding the degree of polarization of the tangle are valid in the limit of both the Kolmogorov and non-cascading

configurations. Open questions are the mechanism of formation of these intense vortical regions, their lifetime, and their eventual dissipation. We plan to address these questions in a future study, using a parallel implementation of the tree approximation.

ACKNOWLEDGMENTS

The author wishes to acknowledge stimulating discussions with Carlo Barenghi and Yuri Sergeev, and the comments of the two anonymous referees.

[1] H. Adachi, S. Fujiyama, and M. Tsubota, "Steady-state counterflow quantum turbulence: Simulation of vortex filaments using the full Biot-Savart law," Phys. Rev. B **81**(10), 104511 (2010).
[2] S. Z. Alamri, A. J. Youd, and C. F. Barenghi, "Reconnection of superfluid vortex bundles," Phys. Rev. Lett. **101**, 215302 (2008).
[3] T. Araki, M. Tsubota, and S. K. Nemirovskii, "Energy spectrum of superfluid turbulence with no normal-fluid component," Phys. Rev. Lett. **89**(14), 145301 (2002).
[4] A. W. Baggaley and C. F. Barenghi, "Tree method for quantum vortex dynamics," J. Low Temp. Phys. **166**, 3–20 (2012).
[5] A. W. Baggaley, "The sensitivity of the vortex filament method to different reconnection models," J. Low Temp. Phys. **168**(1-2), 18 (2012).
[6] A. W. Baggaley and C. F. Barenghi, "Spectrum of turbulent Kelvin-waves cascade in superfluid helium," Phys. Rev. B **83**(13), 134509 (2011).
[7] C. F. Barenghi, R. J. Donnelly, and W. F. Vinen, "Friction on quantized vortices in helium II. A review," J. Low Temp. Phys. **52**, 189–247 (1983).
[8] M. Blakov, M. loveko, E. Gao, L. Skrbek, and P. Skyba, "Quantum turbulence generated and detected by a vibrating quartz fork," J. Low Temp. Phys. **148**, 305–310 (2007).
[9] D. I. Bradley, S. N. Fisher, A. M. Guénault, R. P. Haley, S. O'Sullivan, G. R. Pickett, and V. Tsepelin, "Fluctuations and correlations of pure quantum turbulence in superfluid He-3_ B," Phys. Rev. Lett. **101**(6), 065302 (2008).
[10] T. V. Chagovets and S. W. Van Sciver, "A study of thermal counterflow using particle tracking velocimetry," Phys. Fluids **23**(10), 107102 (2011).
[11] V. B. Eltsov, A. I. Golov, R. de Graaf, R. Hänninen, M. Krusius, V. S. L'vov, and R. E. Solntsev, "Quantum turbulence in a propagating superfluid vortex front," Phys. Rev. Lett. **99**(26), 265301 (2007).
[12] S. Goto, "A physical mechanism of the energy cascade in homogeneous isotropic turbulence," J. Fluid Mech. **605**, 355–366 (2008).
[13] E. A. L. Henn, J. A. Seman, G. Roati, K. M. F. Magalhães, and V. S. Bagnato, "Emergence of turbulence in an oscillating Bose-Einstein condensate," Phys. Rev. Lett. **103**(4), 045301 (2009).
[14] D. Kivotides, J. C. Vassilicos, C. F. Barenghi, M. A. I. Khan, and D. C. Samuels, "Quantum signature of superfluid turbulence," Phys. Rev. Lett. **87**, 275302 (2001).
[15] D. Kivotides, "Coherent structure formation in turbulent thermal superfluids," Phys. Rev. Lett. **96**, 175301 (2006).
[16] J. Koplik and H. Levine, "Vortex reconnection in superfluid helium," Phys. Rev. Lett. **71**(9), 1375–1378 (1993).
[17] E. Kozik and B. Svistunov, "Kolmogorov and kelvin-wave cascades of superfluid turbulence at $t = 0$: What lies between," Phys. Rev. B **77**, 060502 (2008).
[18] V. S. L'vov, S. V. Nazarenko, and O. Rudenko, "Bottleneck crossover between classical and quantum superfluid turbulence," Phys. Rev. B **76**(2), 024520 (2007).
[19] J. Maurer and P. Tabeling, "Local investigation of superfluid turbulence," Europhys. Lett. **43**(1), 29 (1998).
[20] K. Morris, J. Koplik, and D. W. I. Rouson, "Vortex locking in direct numerical simulations of quantum turbulence," Phys. Rev. Lett. **101**(1), 015301 (2008).
[21] D. R. Osborne, J. C. Vassilicos, K. Sung, and J. D. Haigh, "Fundamentals of pair diffusion in kinematic simulations of turbulence," Phys. Rev. E **74**(3), 036309 (2006).
[22] M. S. Paoletti, M. E. Fisher, and D. P. Lathrop, "Reconnection dynamics for quantized vortices," Physica D **239**, 1367 (2010).
[23] P.-E. Roche, C. F. Barenghi, and E. Leveque, "Quantum turbulence at finite temperature: The two-fluids cascade," Europhys. Lett. **87**(5), 54006 (2009).
[24] P. E. Roche, P. Diribarne, T. Didelot, O. Français, L. Rousseau, and H. Willaime, "Vortex density spectrum of quantum turbulence," Europhys. Lett. **77**(6), 66002 (2007).
[25] J. Salort, C. Baudet, B. Castaing, B. Chabaud, F. Daviaud, T. Didelot, P. Diribarne, B. Dubrulle, Y. Gagne, F. Gauthier, A. Girard, B. Hebral, B. Rousset, P. Thibault, and P.-E. Roche, "Turbulent velocity spectra in superfluid flows," Phys. Fluids **22**(12), 125102 (2010).
[26] K. W. Schwarz, "Three-dimensional vortex dynamics in superfluid ^{4}He: Homogeneous superfluid turbulence," Phys. Rev. B **38**(4), 2398–2417 (1988).
[27] L. Skrbek and K. R. Sreenivasan, "Developed quantum turbulence and its decay," Phys. Fluids **24**(1), 011301 (2012).
[28] M. R. Smith, R. J. Donnelly, N. Goldenfeld, and W. F. Vinen, "Decay of vorticity in homogeneous turbulence," Phys. Rev. Lett. **71**(16), 2583–2586 (1993).
[29] J. T. Tough, In *Progress of Low Temperature Physics*, edited by D. F. Brewer (North-Holland, Amsterdam, 1982), Vol. VIII.
[30] W. F. Vinen and J. J. Niemela, "Quantum turbulence," J. Low Temp. Phys. **128**, 167–231 (2002).